Hindawi
Journal of Nanomaterials
Volume 2020, Article ID 6641702, 10 pages
https://doi.org/10.1155/2020/6641702

Research Article

Fabrication and Thermal Degradation Kinetics of PBT/BEO/Nano-Sb_2O_3 Composites

Meng Ma,[1,2,3,4] Lei Niu,[1,4] Jinming Ma,[5] Jiqiang Ma,[4] and Tifeng Jiao[5]

[1]*College of Petrochemical Technology, Lanzhou University of Technology, Lanzhou 730050, China*
[2]*Service Center of Security Production Technology of Gansu Province, Lanzhou 730070, China*
[3]*Emergency Management Information Center of Gansu Province, Lanzhou 730070, China*
[4]*State Key Laboratory of Gansu Advanced Non-Ferrous Metal Materials, Lanzhou University of Technology, Lanzhou 730050, China*
[5]*State Key Laboratory of Metastable Materials Science and Technology, Yanshan University, Qinhuangdao 066004, China*

Correspondence should be addressed to Lei Niu; niulei@lut.cn and Tifeng Jiao; tfjiao@ysu.edu.cn

Received 29 October 2020; Revised 1 December 2020; Accepted 2 December 2020; Published 28 December 2020

Academic Editor: Filippo Giubileo

Developing polybutylene terephthalate (PBT) with high thermal stability and flame-retardant properties is crucial for automotive, biomedical devices, electronics, and other fields. Herein, we focus on a PBT/brominated epoxy resin (BEO)/nano-Sb_2O_3 composites by a melt-blending method. The effects of heating rate and nano-Sb_2O_3 content on the thermal stability and thermal degradation kinetics of PBT composites were studied by TG-DSC. With the increasing of heating rate, the thermal hysteresis effect of temperature gradient is produced, which is eliminated when the temperature exceeds 400°C. With the increase of nano-Sb_2O_3 content, the E_a of PBT/BEO/nano-Sb_2O_3 composites increases at first and then decreases. When the content of nano-Sb_2O_3 is 3 wt%, the E_a of PBT/BEO/nano-Sb_2O_3 is the highest, which is 66.18 kJ/mol (31.43%) higher than that of neat PBT. Also, the exploration of the thermal degradation kinetics of PBT/BEO/nano-Sb_2O_3 composites is expected to provide research ideas for new high flame-retardant materials.

1. Introduction

As a semicrystalline thermoplastic polymer, polybutylene terephthalate (PBT) possessed excellent mechanical properties and thermal property, which is widely used in engineering fields such as automobile, biomedical devices, and electronic and electrical industry [1, 2]. But PBT is mainly composed of carbon and hydrogen, which leads to strong flammability and serious dripping as it burned. It is currently in the compound use of several flame retardants to improve thermal stability and flame retardancy for PBT composites [3]. However, these additive flame retardants are seriously affecting the mechanical properties and restricting the application of PBT composite. Therefore, the development of PBT composites with comprehensive physical and mechanical properties, thermal stability, and flame-retardant properties has become the keys to expand their application.

Nanometal oxide materials exhibit an unparalleled combination of chemical, electrical, magnetic, optical, and thermal properties [4, 5], which have potential applications in flame retardants, electronics, and photonics industry. Sb_2O_3 is one of nanometal oxides with excellent performance, which is often used as a flame-retarding additive for various plastics, rubber, and polymer materials [6]. Wang et al. reported the effect of $MnCo_2O_4$-GNS hybrid on PBT thermal degradation, and they concluded that the thermal stability of $MnCo_2O_4$-GNS/PBT composite improved greatly [7]. Feng et al. researched the thermal performance for polysulfonamide-based single polymer composites (PSA/SPCs) by thermogravimetric analysis (TG), and the results showed that thermal stability of PSA/SPCs was better than PSA resin composite [8]. Wang et al. investigated that the heating oxidation behaviors for short glass fiber reinforced nylon composite filled with brominated epoxy resin (BEO)/Sb_2O_3; they concluded that the thermal stability of the composite was improved after aging at 160°C for 50 days, but after aging at 200°C for 50 days, the structure of the composite was seriously damaged and the

Table 1: The composite material content of the component (wt%).

Sample	BEO	Nano-Sb_2O_3	PBT
Neat PBT	0	0	100
PBT/BEO	16	0	94.0
PBT/BEO/nano-Sb_2O_3 1 wt%	16	1.0	93.0
PBT/BEO/nano-Sb_2O_3 3 wt%	16	3.0	91.0
PBT/BEO/nano-Sb_2O_3 5 wt%	16	5.0	89.0

thermal degradation behavior changed significantly [9]. Studies have shown that adding epoxy resin-coated ammonium polyphosphate microcapsules into polypropylene could increase the activation energy of polypropylene from 100.8 kJ/mol to 127.5 kJ/mol [10]. Qi et al. reported that aluminum hypophosphite/reduced graphene oxide (AHP/RGO) was added to the PBT matrix that could significantly reduce the heat release of the composites and improve the thermal stability and antidripping property of composites [11]. Many efforts have been made to develop the PBT composites with high thermal stability and flame-retardant properties. However, few studies focused on the effects of BEO and nano-Sb_2O_3 on the thermal degradation of PBT. In addition, there is a correlation between the thermal stability and flame retardancy of nanocomposites. Therefore, it is also of great significance to study the thermal degradation kinetics of composites for improving its comprehensive properties.

In this paper, the PBT/BEO/nano-Sb_2O_3 composites were prepared via methods of melt-mixing and injection molding. The effects of heating rate and nano-Sb_2O_3 content on the thermal stability and thermal degradation kinetics of PBT composites were studied. With the increase of nano-Sb_2O_3 particle content, the peak value of the thermal degradation rate of PBT composites gradually decreases, the thermal stability performance gradually improves, and the carbon residue rate also increases significantly.

2. Materials and Methods

2.1. Materials. Poly(butylene terephthalate) (PBT, 1100-211M), with a density of 1.31 g/cm^3, was provided by Taiwan Chang Chun Plastics Co., Ltd., Suzhou, China. Nano-Sb_2O_3 was prepared and modified by ball milling, as reported in our study [12–14]. The particle size was 50-100 nm. Brominated epoxy resin (BEO, with an average weight of 20,000 and a bromine content of 53.2%) was provided by BASF Chemical Co., Shanghai, China. Cetyltrimethylammonium bromide (CTAB) was produced by Shanghai Zhongqin Chemical Reagent Co., Ltd. Silane coupling agent (KH550) was provided by Sinopharm Chemical Reagent Co., Ltd.

Powders of PBT, BEO, and nano-Sb_2O_3 particles were treated by ball milling at the conditions of revolving velocity which was 400 r/min for 6 hours to maintain better dispersion. BEO, nano-Sb_2O_3, and PBT were mixed with different mass ratios; mixtures were added into the extruder for melt blending and then into the injection machine. Mixture melts were injected into a model to prepare specimens. The component contents of specimens are listed in Table 1.

2.2. Characterization. PBT composites were treated by spray-gold. The JSM 6700 Scanning Electron Microscope (SEM) was used to study the microstructure of specimens. Thermodynamic behavior was investigated with Mettler Toledo Thermogravimetric Analysis (TG-DSC). In the experiments, the range of quality was 5~10 mg. Specimens were heated from room temperature to 600°C; heating rates were 5°C/min, 10°C/min, 20°C/min, and 40°C/min.

3. Results and Discussion

3.1. Thermal Stability of PBT/BEO/Nano-Sb_2O_3 Composites

3.1.1. Thermal Stability Effects of Heating Rates on PBT Composites. Curves of TG and DTG for pure PBT are shown in Figures 1(a) and 1(b), the heating rates at 5°C/min, 10°C/min, 20°C/min, and 40°C/min. As shown in Figure 1, the temperature of initial decomposition, maximum decomposition rate, and thermal weight loss rate of pure PBT all move to high temperature with the increase of heating rate. However, the heating rate has little effect on the final thermal decomposition of pure PBT, and the TG trends of the four curves have not changed. The main reason for this phenomenon is that the temperature variation changes between furnace and specimens with the increasing heating rate and the temperature gradient are generated in the internal of specimens.

Figure 2 shows the TG-DSC curves of pure PBT at the heating rate of 5°C/min (Figure 2(a)), 10°C/min (Figure 2(b)), 20°C/min (Figure 2(c)), and 40°C/min (Figure 2(d)). There are two endothermic peaks in the TG-DSC curves of pure PBT. The first endothermic peak appears in the range of 223~226°C. However, there is no corresponding weight loss on the TG. The endothermic peak in this range is the phase transition endothermic peak of neat PBT from solid to liquid, and PBT composites do not begin to break and decompose. Different heating rates have no effect on the phase transition temperature of PBT. The second endothermic peak appears at the temperature of around 400°C; there is a significant thermal degradation process. The main chain of PBT begins to break down into polymer fragments, then further produces small molecule combustible gases, and escapes small molecule combustible gases. As the heating rate increases, the endothermic peak gradually shifts to a higher temperature, which is consistent with the DTG curve of neat PBT (Figure 1(b)).

The maximum degradation rate of pure PBT is about 400°C; the obvious rapid degradation process occurred. With the increase of heating rate, the carbon residue rate increases gradually in the range of 350°C to 400°C. This shows that with the increase of heating rate, the thermal degradation of PBT also has a hysteresis effect due to the thermal hysteresis effect of the temperature gradient. When the temperature exceeds 400°C, the thermal hysteresis effect is gradually eliminated. With the increase of heating rate, the thermal stability of PBT decreases, the decomposition rate of PBT increases correspondingly, and the residual carbon rate decreases.

3.1.2. Thermal Stability Effects of Heating Rates on PBT/BEO Composites. The TG and DTG curves of PBT/BEO composites with 16 wt% BEO flame retardant at different heating

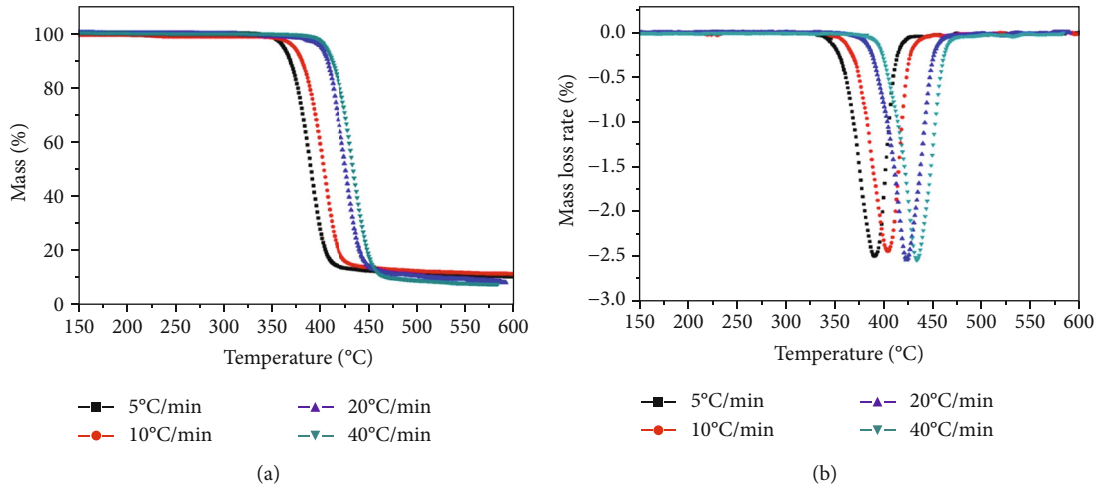

Figure 1: TG (a) and DTG (b) curves of pure PBT at different heating rates.

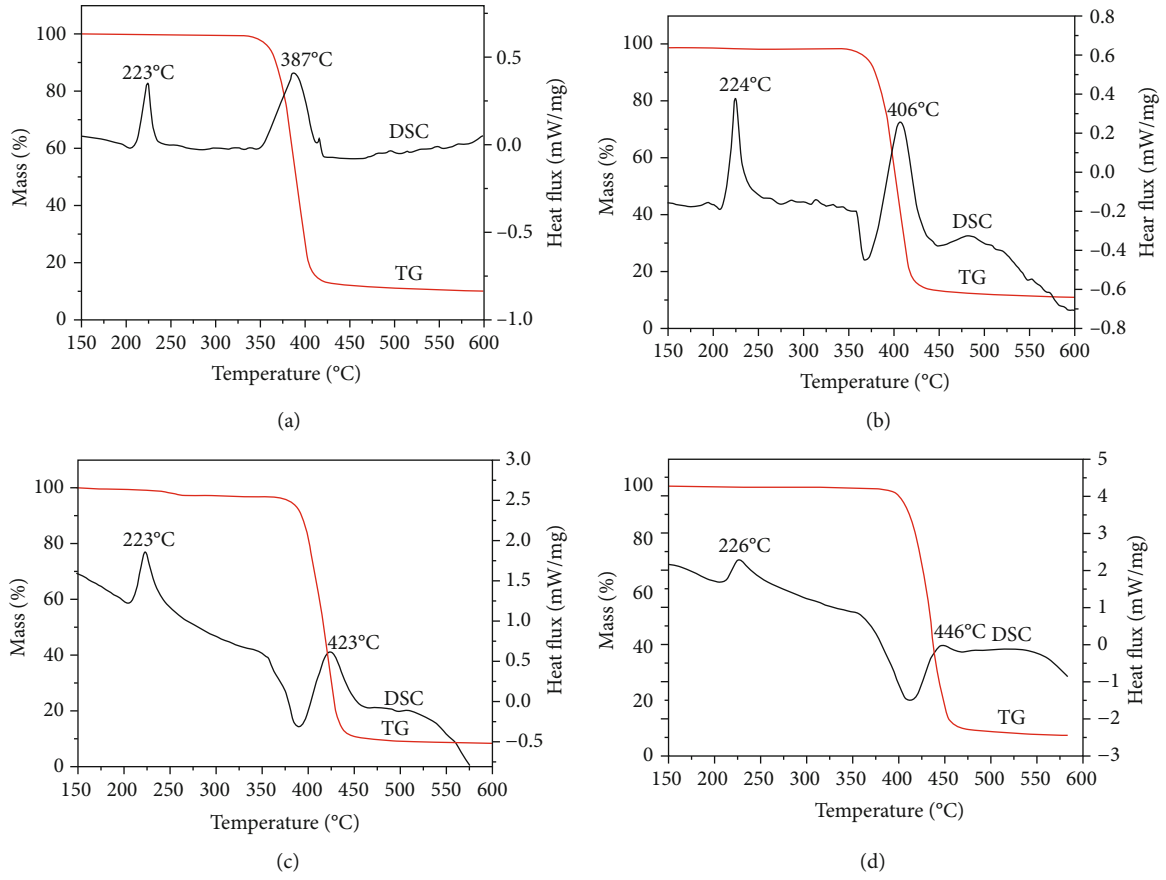

Figure 2: TG-DSC curves of pure PBT at different heating rates: (a) 5°C/min, (b) 10°C/min, (c) 20°C/min, and (d) 40°C/min.

rates are shown in Figure 3. There are two endothermic peaks at different heating rates in all pictures. With the addition of BEO flame retardants, the trend of thermal degradation does not change. The DTG curves still have a symmetrical single peak. The results show that the BEO flame retardant has good compatibility with the PBT matrix. The addition of BEO flame retardants reduces the thermal degradation rate of PBT composites and improves the thermal stability of PBT, which is beneficial to improve the flame retardancy of PBT/BEO composites. The initial degradation temperature of the PBT/BEO composite is reduced, and the molecular chain of PBT/BEO composite breaks down earlier. However, the maximum thermal degradation temperature of PBT/BEO composites is still around 400°C. With the increase of heating rate, the thermal degradation trend of PBT/BEO composites is consistent with that of pure PBT.

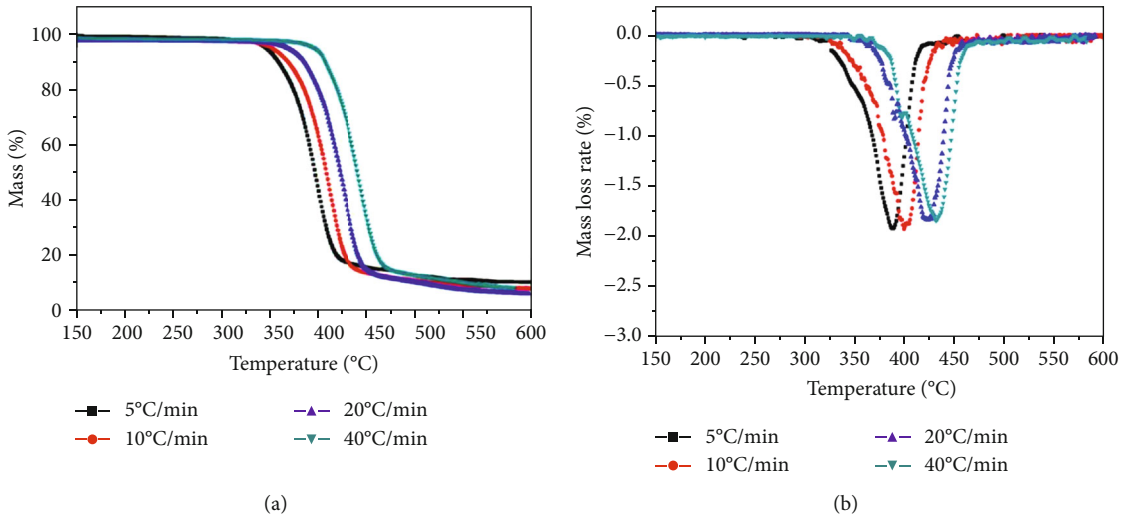

Figure 3: TG (a) and DTG (b) curves of PBT/BEO (16 wt% BEO) composites at different heating rates.

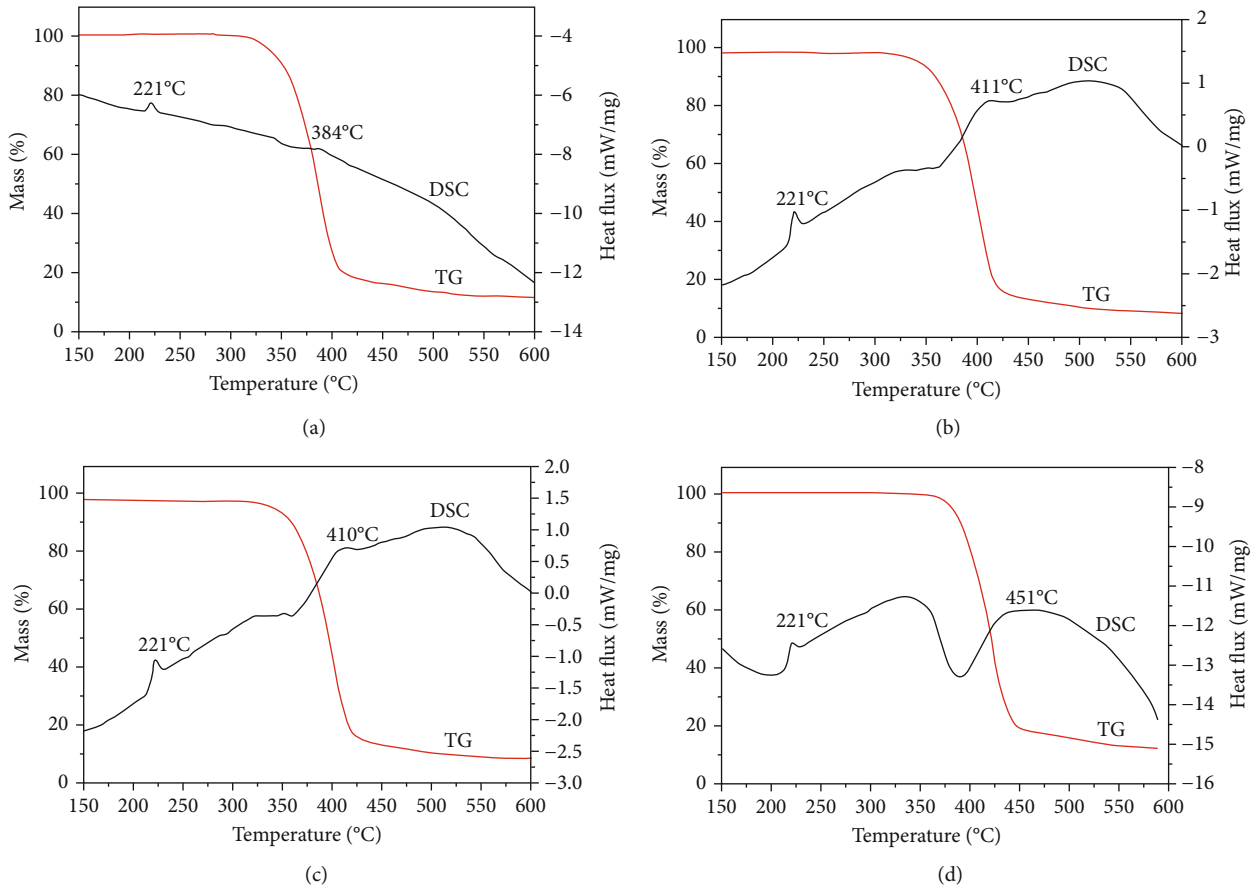

Figure 4: TG-DSC curves of PBT/BEO composites at different heating rates: (a) 5°C/min, (b) 10°C/min, (c) 20°C/min, and (d) 40°C/min.

TG-DSC curves of PBT/BEO composite at four kinds of heating rate are illustrated in Figure 4. Each of the four TG-DSC curves at different heating rates has endothermic peak values, and the first phase transition endothermic peak of which appears at 221°C, indicating that the phase-change temperature is not affected by heating rate. The second endothermic peak appears at about 400°C, and the TG process is evident at this stage. The endothermic peak temperature gradually shifts to high temperature with the increase of heating rate, which is basically consistent with the TG-DSC curve of neat PBT.

3.1.3. Thermal Stability Effects of Heating Rates on PBT/BEO/Nano-Sb_2O_3 Composites. To further improve the

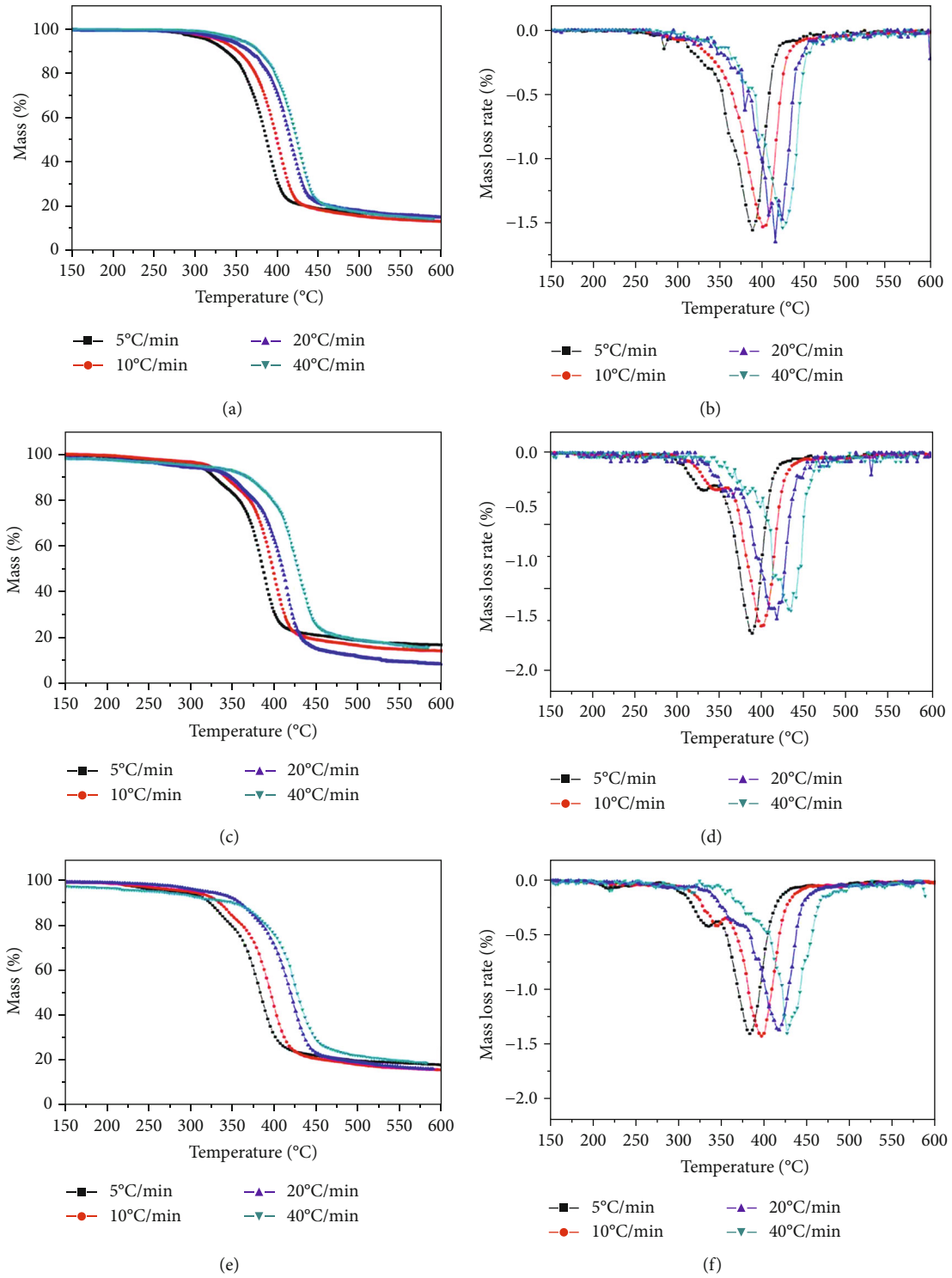

Figure 5: TG (a, c, e) and DTG (b, d, f) curves of PBT/BEO/nano-Sb_2O_3 composites (1 wt%, 3 wt%, and 5 wt% contents of nano-Sb_2O_3) at different heating rates.

thermal stability and flame-retardant properties of PBT/BEO, 1 wt%, 3 wt%, and 5 wt% contents of nano-Sb_2O_3 synergistic flame retardant were added to the PBT/BEO composites, forming PBT/BEO/nano-Sb_2O_3 x wt% (x = 1, 3, 5) composites. The TG and DTG curves of the three kinds of PBT/BEO/nano-Sb_2O_3 composites are shown in Figure 5, at different heating rates. The TG curves and temperature excursion trends of PBT/BEO/nano-Sb_2O_3 composites are similar to that of the PBT/BEO composite. However, with the addition of nano-Sb_2O_3, the peak values of TG decrease significantly. When the content of nano-Sb_2O_3 reaches more than 3 wt%, a phenomenon can be found by comparing Figures 1 and 3.

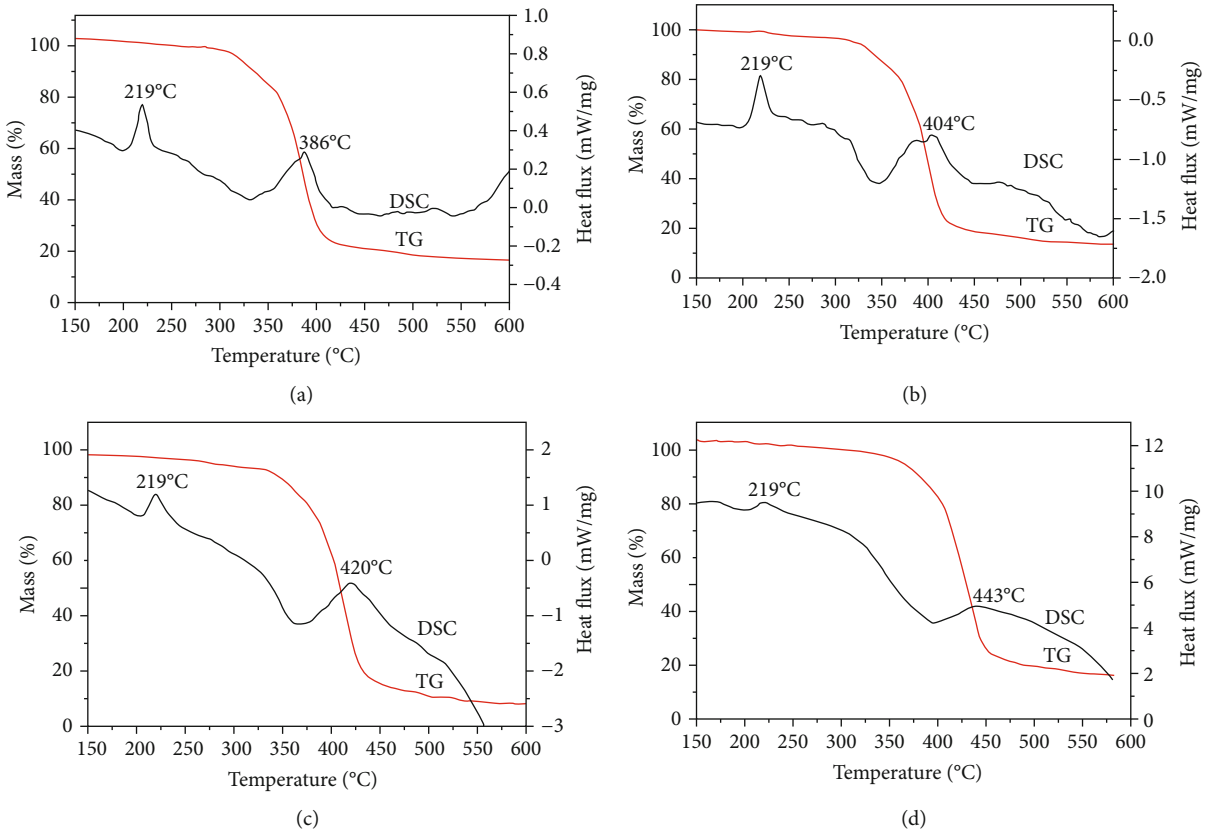

Figure 6: TG-DSC curves of PBT/BEO/nano-Sb_2O_3 3 wt% composites at different heating rates: (a) 5°C/min, (b) 10°C/min, (c) 20°C/min, and (d) 40°C/min.

A slowing band of the thermal degradation rate appears in DTG curves near 320°C, which prevents further thermal degradation of PBT composites. It indicates that there is a synergistic effect between BEO and nano-Sb_2O_3 after the addition of 3 wt% nano-Sb_2O_3. In the early stage of PBT/BEO/nano-Sb_2O_3 composite pyrolysis, coflame retardants play a role, improving the thermal stability of PBT/BEO/nano-Sb_2O_3 composites and the flame-retardant properties at the initial stage of combustion.

The representative PBT/BEO/nano-Sb_2O_3 3 wt% composite was selected to study the effect of heating rate on the thermal stability of the PBT composite. As the heating rate increases, the thermal degradation trend of PBT/BEO/-nano-Sb_2O_3 3 wt% composite is similar to that of PBT/BEO. The results show that the addition of nano-Sb_2O_3 does not change the thermal degradation process of PBT/BEO composites but improves the thermal stability of PBT/BEO composites, and the carbon residue rate increases significantly. The TG-DSC curves of PBT/BEO/nano-Sb_2O_3 3 wt% composites at different heating rates are shown in Figure 6. At high heating rates, peak fluctuations are not obvious. The DSC curve peak of the PBT/BEO/nano-Sb_2O_3 3 wt% composite is similar to that of the PBT/BEO composite. The endothermic peak temperature gradually shifts to high temperatures with an increase in heating rate.

3.1.4. Effect of Nano-Sb_2O_3 Content on the Thermal Stability of PBT Composites. To study the effect of nano-Sb_2O_3 content on the thermal stability of PBT composites, the thermal stability properties of neat PBT and its composites were tested at 600°C with a heating rate of 5°C/min; the corresponding thermal performance data are summarized in Table 2. TG and DTG curves of neat PBT and its composites at a heating rate of 5°C/min are presented in Figure 7. The results show that the PBT composites still have a single weight-loss stage, and the DTG curves have only one large weight loss peak after adding BEO and nano-Sb_2O_3 particles from Table 2 and Figure 7. This indicates that the thermal degradation process of PBT composite is mainly the catalytic fracture of the primary key. However, the thermal degradation of neat PBT and its composites can be divided into two stages: a rapid decomposition stage and a slow degradation stage of a stable carbon layer.

Table 2: Thermal properties of pure PBT and its composites at a heating rate of 5°C/min.

No.	Specimens	$T_{10\%}$ (°C)	T_{peak} (°C)	600°C carbon residue rate (%)
1	Neat PBT	367.5	389.7	10.10
2	PBT/BEO	349.3	389.5	10.55
3	PBT/BEO/nano-Sb_2O_3 1 wt%	341.7	389.6	13.92
4	PBT/BEO/nano-Sb_2O_3 3 wt%	336.6	386.8	16.42
5	PBT/BEO/nano-Sb_2O_3 5 wt%	323.4	382.8	17.23

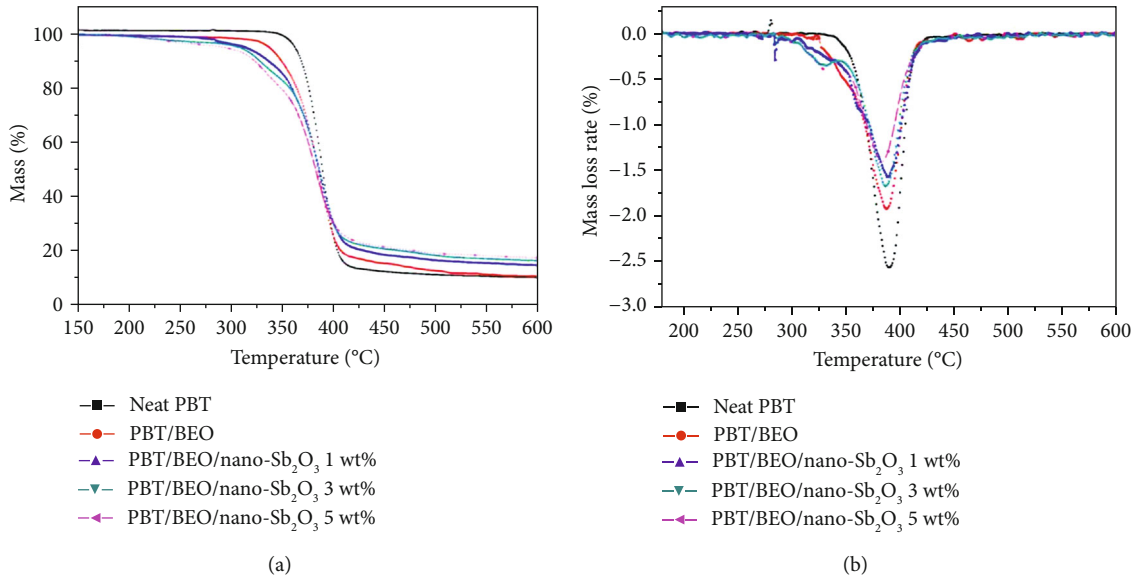

Figure 7: TG (a) and DTG (b) curves of pure PBT and its composites.

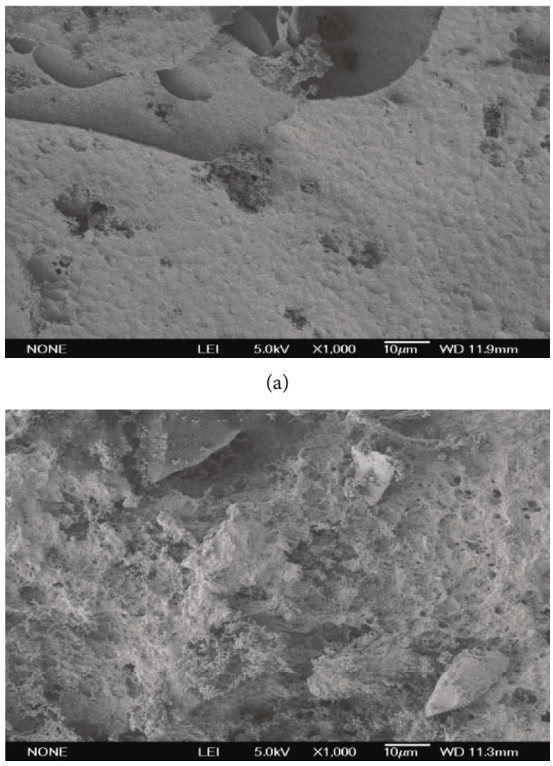

Figure 8: SEM images of (a) pure PBT; (b) PBT/BEO/nano-Sb_2O_3 3 wt%.

The first stage mainly occurs between 320°C and 430°C. The initial decomposition temperature of nano-Sb_2O_3 particles occurs during the slow degradation stage of the PBT stable carbon layer. After adding the BEO flame retardant, the thermal decomposition temperature of the PBT composite is increased, and the carbon residue rate is improved. With the addition of nano-Sb_2O_3 in different contents, the initial

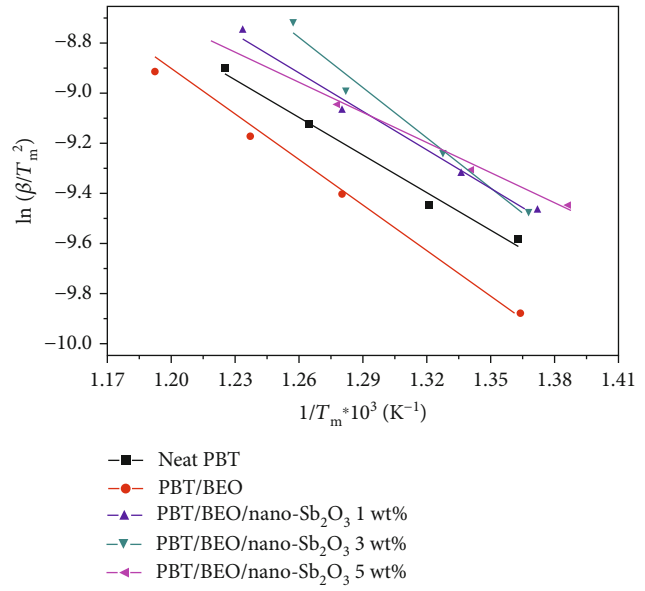

Figure 9: ln (β/T_m^2) and $1/T_m$ relation diagram of pure PBT and its composites.

decomposition temperature ($T_{10\%}$) of PBT/BEO/nano-Sb_2O_3 composites is decreased by 25.8°C (1 wt%), 30.9°C (3 wt%), and 44.1°C (5 wt%) compared to the pure PBT, respectively (Table 2). With the increase of nano-Sb_2O_3 content, the maximum thermal decomposition peak temperature and thermal decomposition rate of PBT/BEO/nano-Sb_2O_3 composites decreased gradually. This may be due to the catalytic effect of metal oxides on macromolecular chain cleavage, which promotes the rapid oxidation of PBT matrix materials [15]. The interaction between nano-Sb_2O_3 and BEO flame retardants and PBT matrix materials promotes the thermal decomposition of PBT composites at lower temperatures, resulting in the formation of some high-quality carbon residue layers. At this stage, the high-temperature

Table 3: Activation energy E_a and frequent factors lnA are calculated by the Kissinger method.

Specimens	T_m (°C/min) 5	10	20	40	Correlation coefficient	Activation energy E_a (kJ/mol)	Frequent factors lnA
Neat PBT	389.7	402.8	421.5	431.8	0.9802	210.56	23.4
PBT/BEO	389.5	416.3	431.1	448.1	0.9909	233.28	23.6
PBT/BEO/nano-Sb_2O_3 1 wt%	388.5	400.7	415.5	424.0	0.9788	264.21	25.1
PBT/BEO/nano-Sb_2O_3 3 wt%	387.3	398.2	416.1	432.5	0.9898	276.74	24.2

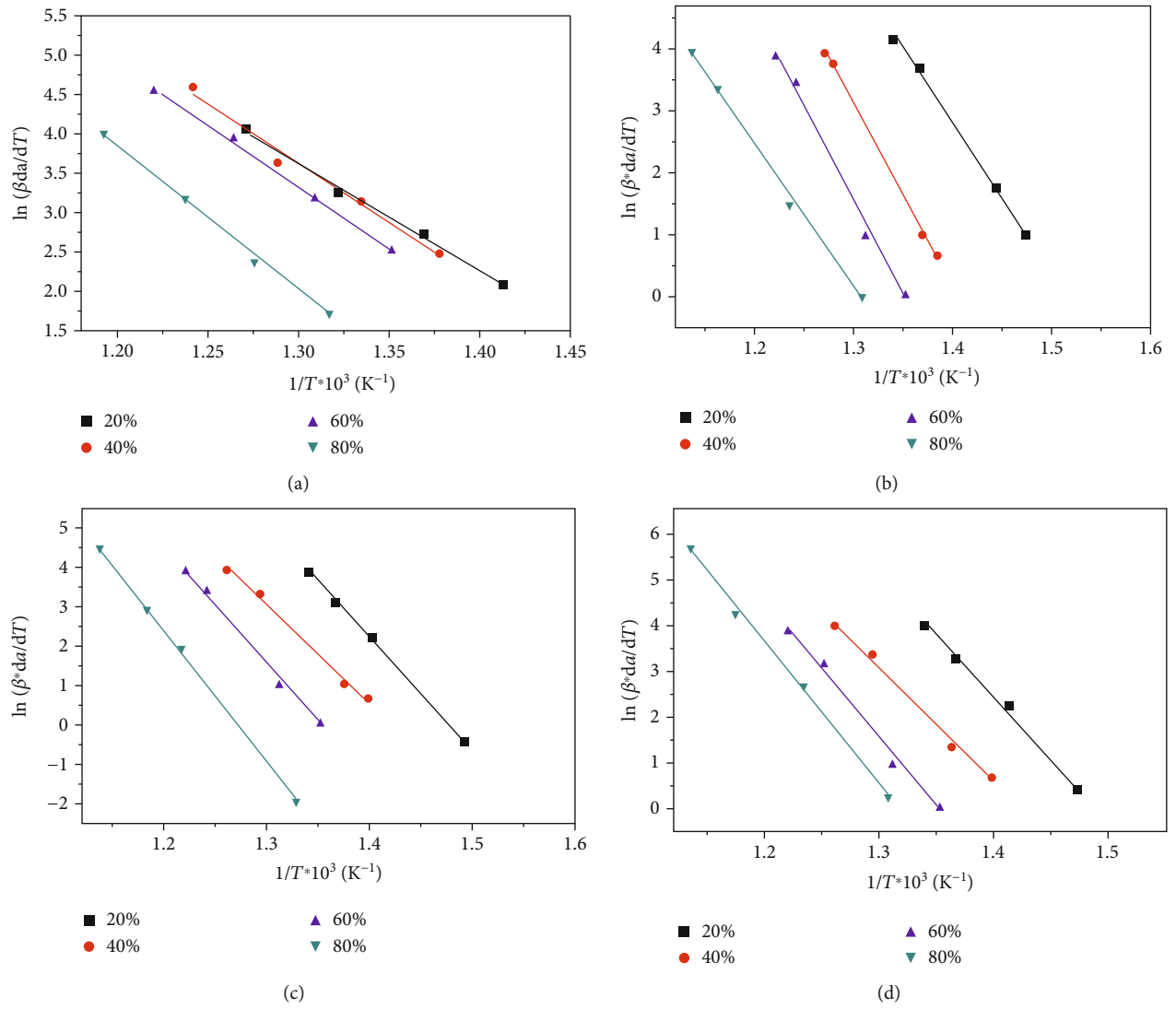

Figure 10: $\ln(\beta/T_m^2)$ and $(1/T_m) * 10^3$ relationship diagram of pure PBT and its composites. (a) Neat PBT; (b–d) PBT/BEO/nano-Sb_2O_3 composites (1 wt%, 3 wt%, and 5 wt% contents of nano-Sb_2O_3).

heat energy promotes the cleavage of various bonds in the molecular chain of PBT materials. As a result of the degradation of bond cleavage, the mass loss of polymers increases rapidly, which is reflected in the TG and DTG curves.

In the second stage, with the increase of pyrolysis temperature, the initial carbon layer of PBT composites is gradually decomposed, but the residual amount of PBT composites is still higher than that of neat PBT material. Studies show that the effective carbonization process of flame-retardant polymer materials occurs at a temperature higher than the processing temperature, but much lower than the decomposition temperature of the polymer matrix material [16]. Therefore, in the first stage of degradation, the effective carbonization layer is formed by the early pyrolysis of PBT composites. It is beneficial to delay the thermal degradation of PBT matrix materials in a higher temperature range and improve the thermal stability and flame-retardant properties of PBT composites. Table 2 indicates that the carbon

Table 4: Reaction kinetic parameters are calculated by the Friedman method.

Specimens	Correlation coefficient	Activation energy E_a (kJ/mol)	Reaction order
Neat PBT	0.9934	195.98	0.89
PBT/BEO/nano-Sb_2O_3 1 wt%	0.9942	253.72	0.92
PBT/BEO/nano-Sb_2O_3 3 wt%	0.9953	267.94	0.95
PBT/BEO/nano-Sb_2O_3 5 wt%	0.9952	258.97	0.91

residue rate of neat PBT is 10.1 wt% at 600°C, while the carbon residue rate of neat PBT increased significantly 0.45% after adding 16 wt% BEO flame retardant. After adding nano-Sb_2O_3 particles, the residual carbon rate increased significantly. The results show that there is a synergistic effect between BEO and nano-Sb_2O_3 particles, and nano-Sb_2O_3 particles change the thermal degradation mechanism of PBT. With the increase of nano-Sb_2O_3 content, the peak value of the thermal degradation rate of the PBT composite decreases gradually. The results show that bromine antimony synergistic flame retardant effectively delays the thermal degradation of PBT matrix materials. BEO and nano-Sb_2O_3 can promote the carbonization of PBT during the combustion process, resulting in a significant increase in the residual carbon rate.

To further analyze the relationship between nano-Sb_2O_3 content and thermal stability of PBT/BEO/nano-Sb_2O_3 composites, the surface morphology SEM images of solid residues of neat PBT (Figure 8(a)) and PBT/BEO/nano-Sb_2O_3 3 wt% (Figure 8(b)) after combustion are shown in Figure 8. Compared with neat PBT, a large number of lamellar and agglomerate structures appear on the surface of solid residue after the combustion of PBT/BEO/nano-Sb_2O_3 3 wt%, forming a protective film with a network structure. This kind of network barrier structure can hinder the conduction of combustible volatiles and heat produced in the thermal degradation process of PBT composites and protects the thermal degradation of PBT.

3.2. Kinetic Parameters of Nano-Sb_2O_3/BEO/PBT Composites. The Kissinger method and Friedman method were used to calculate the thermal degradation kinetic parameters of the composites. The straight lines of composite materials calculated by the Kissinger method are demonstrated in Figure 9. The activation energy E_a and frequent factors lnA were calculated according to the slope and intercept of the straight line which are summarized in Table 3. At the heating rate of 10°C/min and 40°C/min, the critical transition temperature of the neat PBT is 402.8°C and 431.8°C, respectively. After adding 3 wt% nano-Sb_2O_3 particles into PBT/BEO, the critical transition temperature of PBT/BEO/nano-Sb_2O_3 3 wt% is 398.2°C at the heating rate of 10°C/min, and the transition temperature is reduced by about 5°C. Here, nano-Sb_2O_3 particles have a catalytic effect on the molecular chain of PBT. It can be seen from Figure 9 and Table 3 that the addition of nano-Sb_2O_3 particles has a certain effect on the thermal stability of PBT. With the increase of nano-Sb_2O_3 content, the E_a of PBT composites increases at first and then decreases. When the content of nano-Sb_2O_3 is 3 wt%, the E_a is the highest, which is 66.18 kJ/mol (31.43%) higher than that of pure PBT. At this time, the thermal degradation of PBT composites is the most difficult, which indicates that the addition of nano-Sb_2O_3 particles hinders the movement of molecular chains and enhances the thermal stability of PBT.

The degradation kinetic parameters E_a and reaction order n obtained by the Friedman method are shown in Figure 10 and Table 4. It can be seen from Table 4 that the thermal degradation of the PBT composites belongs to the first-order reaction. With the increase of nano-Sb_2O_3 content, the activation energy of thermal degradation first increases and then decreases, which is consistent with the change rule of activation energy obtained by the Kissinger method. When the content of nano-Sb_2O_3 is 3 wt%, the activation energy E_a increased by 71.96 kJ/mol (36.72%) compare with neat PBT. From the increase of activation energy E_a value, it can be seen that there is an interaction between nanofiller and PBT matrix material, which reduces the movement of distal chain in PBT nanocomposites and improves its thermal stability [17].

The thermal degradation reaction of PBT can be regarded as zero order in the early stage, and the degradation reaction under a high weightlessness rate can be regarded as the first order [18–24]. The thermal degradation of pure PBT and its composites can be divided into two stages. In the early stage of the reaction, the reaction order is zero. With the increase of thermal degradation temperature, the reaction order changes from zero to the first order in the second stage.

4. Conclusions

With the increase of heating rate, the thermal hysteresis effect of the temperature gradient is produced, and the thermal degradation of PBT composite also has a hysteresis effect. When the temperature exceeds 400°C, the thermal hysteresis effect is gradually eliminated. With the increase of nano-Sb_2O_3 particle content, the thermal degradation activation energy E_a of PBT/BEO/nano-Sb_2O_3 increases at first then decreases, and its maximum value at 3 wt% nano-Sb_2O_3. The results indicate that the addition of nano-Sb_2O_3 particles hinders the movement and regular stacking of molecular chains. Therefore, the BEO and nano-Sb_2O_3 particles can enhance the thermal stability of PBT and increase the maximum activation energy of thermal degradation.

Data Availability

The data used to support the findings of this study are available from the corresponding authors upon request.

Conflicts of Interest

The authors report no conflicts of interest in this work.

Authors' Contributions

Lei Niu and Tifeng Jiao conceived and designed the experiments; Meng Ma and Jiqiang Ma performed the experiments; Tifeng Jiao analyzed the data; Meng Ma, Jiqiang Ma, and Lei Niu contributed reagents/materials/analysis tools; Jinming Ma and Tifeng Jiao wrote and revised the paper.

Acknowledgments

This work was supported by the National Natural Science Foundation of China (Nos. 21872119 and 22072127).

References

[1] S. Brehme, T. Köppl, B. Schartel et al., "Phosphorus polyester - an alternative to low-molecular-weight flame retardants in poly(butylene terephthalate)?," *Macromolecular Chemistry and Physics*, vol. 213, no. 22, pp. 2386–2397, 2012.

[2] D. H. Zhang, M. He, W. D. He, Y. Zhou, S. Qin, and J. Yu, "Influence of thermo-oxidative ageing on the thermal and dynamical mechanical properties of long glass fibre-reinforced poly(butylene terephthalate) composites filled with DOPO," *Materials*, vol. 10, no. 5, p. 500, 2017.

[3] U. Braun, H. Bahr, H. Sturm, and B. Schartel, "Flame retardancy mechanisms of metal phosphinates and metal phosphinates in combination with melamine cyanurate in glass-fiber reinforced poly(1,4-butylene terephthalate): the influence of metal cation," *Polymers for Advanced Technologies*, vol. 19, no. 6, pp. 680–692, 2008.

[4] X. Wang, W. Y. Xing, X. M. Feng et al., "The effect of metal oxide decorated graphene hybrids on the improved thermal stability and the reduced smoke toxicity in epoxy resins," *Chemical Engineering Journal*, vol. 250, pp. 214–221, 2014.

[5] T. Metanawin, A. Jamjumrus, and S. Metanawin, "Morphology, mechanical and thermal properties of PBT-TiO2Polymer nanocomposite," *MATEC Web of Conference*, vol. 30, p. 01012, 2015.

[6] M. M. Si, J. Feng, J. W. Hao, L. S. Xu, and J. X. Du, "Synergistic flame retardant effects and mechanisms of nano- Sb_2O_3 in combination with aluminum phosphinate in poly(ethylene terephthalate)," *Polymer Degradation and Stability*, vol. 100, pp. 70–78, 2014.

[7] D. Wang, Q. J. Zhang, K. Q. Zhou, W. Yang, Y. Hu, and X. L. Gong, "The influence of manganese-cobalt oxide/graphene on reducing fire hazards of poly(butylene terephthalate)," *Journal of Hazardous Materials*, vol. 278, pp. 391–400, 2014.

[8] B. Feng, M. Yu, J. Ji, L. Liu, M. Ren, and J. Sun, "Thermal properties and thermal degradation kinetics of polysulfonamide based single polymer composites," *Polymer Materials Science and Engineering*, vol. 32, no. 3, pp. 42–47, 2016.

[9] M. Wang, H. Song, W. He, J. Wang, D. Zhou, and J. Guo, "Thermal oxidation and thermal degradation kinetics of brominated epoxy resin/Sb2O3flame retardant PA10T/GF composites," *Polymer Engineering & Science*, vol. 58, no. 9, pp. 1583–1595, 2018.

[10] C. Liu, K. Chen, L. Ji, and J. Zhu, "Preparation of epoxy resin coated ammonium polyphosphate microcapsules and their flame retardant effects on polypropylene," *Acta Materiae Compositae Sinica*, vol. 3, no. 32, pp. 728–736, 2015.

[11] Y. X. Qi, W. H. Wu, X. W. Liu, H. Q. Qu, and J. Z. Xu, "Preparation and characterization of aluminum hypophosphite/reduced graphene oxide hybrid material as a flame retardant additive for PBT," *Fire and Materials*, vol. 41, no. 3, pp. 195–208, 2017.

[12] L. Niu, J. L. Xu, W. L. Yang, C. H. Kang, J. Q. Ma, and J. Q. Su, "Synergistic effect between nano-Sb2O3and brominated epoxy resin on the flame retardancy of poly(butylene terephthalate)," *Science of Advanced Materials*, vol. 11, no. 4, pp. 466–475, 2019.

[13] L. Niu, J. L. Xu, W. L. Yang, B. X. Ma, and C. H. Kang, "Crystallization, flame retardancy and mechanical properties of poly(butylene terephthalate)/brominated epoxy/nano-Sb2O3-composites dispersed by high energy ball milling," *Journal of Macromolecular Science, Part B*, vol. 57, no. 8, pp. 572–584, 2018.

[14] L. Niu, J. Xu, W. Yang et al., "Study on the synergetic fire-retardant effect of nano-Sb_2O_3 in PBT matrix," *Materials*, vol. 11, no. 7, p. 1060, 2018.

[15] G. S. Deshmukh, D. R. Peshwe, S. U. Pathak, and J. D. Ekhe, "A study on effect of mineral additions on the mechanical, thermal, and structural properties of poly(butylene terephthalate) (PBT) composites," *Journal of Polymer Research*, vol. 18, no. 5, pp. 1081–1090, 2011.

[16] H. Abe, "Thermal degradation of environmentally degradable poly (hydroxyalkanoic acid)s," *Macromolecular Bioscience*, vol. 6, no. 7, pp. 469–486, 2006.

[17] X.-L. Xie, Q.-X. Liu, R. K.-Y. Li et al., "Rheological and mechanical properties of PVC/$CaCO_3$ nanocomposites prepared by in situ polymerization," *Polymer*, vol. 45, no. 19, pp. 6665–6673, 2004.

[18] C. Qian, R. Wang, M. Li et al., "Facile preparation of self-assembled black phosphorus-based composite LB films as new chemical gas sensors," *Colloids and Surfaces A: Physicochemical and Engineering Aspects*, vol. 608, p. 125616, 2021.

[19] J. Bai, R. Wang, M. Ju, J. Zhou, L. Zhang, and T. Jiao, "*Facile preparation and high performance of wearable strain sensors based on ionically cross-linked composite hydrogels*," *Science China Materials*, 2020.

[20] M. Cao, Y. Shen, Z. Yan et al., "Extraction-like removal of organic dyes from polluted water by the graphene oxide/PNIPAM composite system," *Chemical Engineering Journal*, vol. 405, p. 126647, 2021.

[21] J. Zhu, X. Zhang, Z. Qin et al., "Preparation of PdNPs doped chitosan-based composite hydrogels as highly efficient catalysts for reduction of 4-nitrophenol," *Colloids and Surfaces A: Physicochemical and Engineering Aspects*, p. 125889, 2020.

[22] C. Qian, J. Yin, J. Zhao et al., "Facile preparation and highly efficient photodegradation performances of self- assembled Artemia eggshell-ZnO nanocomposites for wastewater treatment," *Colloids and Surfaces A: Physicochemical and Engineering Aspects*, p. 125752, 2020.

[23] M. Wang, Z. Shang, X. Yan et al., "Enhance fluorescence study of grating structure based on three kinds of optical disks," *Optics Communications*, vol. 481, p. 126522, 2021.

[24] R. Su, H. Wang, Y. Sun, and P. Guo, "Structural regulation of porous MnO_2 nanosheets and their electrocapacitive behavior in aqueous electrolytes," *Colloids and Surfaces A: Physicochemical and Engineering Aspects*, vol. 609, p. 125579, 2021.